American Mineralogist, Volume 77, pages 1242–1249, 1992

Sieve-textured plagioclase in volcanic rocks produced by rapid decompression

STEPHEN T. NELSON, ART MONTANA*
Department of Earth and Space Sciences, UCLA, Los Angeles, California 90024-1567, U.S.A.

ABSTRACT

Disequilibrium textures, particularly the coarse sieve texture of plagioclase, are common in orogenic volcanic rocks. The textures are usually interpreted as resulting from magma mixing, but they may occur by rapid decompression, where heat loss is minor relative to the ascent rate. We conducted high-pressure piston-cylinder experiments on an andesite to test this hypothesis. Experiments starting at 12 kbar, followed by isothermal pressure release in increments of 2, 4, and 6 kbar, produce sieve textures in plagioclase very much like those in many volcanic rocks. Therefore, the presence of sieve-textured plagioclase should not be taken as a priori evidence for magma mixing. Many volcanic systems probably experience conditions of decompression similar to those simulated in this study, and decompression is considered to be a simple mechanism to produce such textures, as it requires no addition of heat or mass. Rapid decompression may also operate in conjunction with magma mixing.

INTRODUCTION

Plagioclase commonly exhibits a variety of disequilibrium textures in volcanic rocks, especially in orogenic andesites. These textures often include combinations of complex zoning patterns and resorption features in plagioclase that record changing physical conditions in magmatic systems. Thus, the potential exists to learn much about magmatic processes involved in their formation if the textures can be interpreted, with the caveat that erroneous inferences may result if a particular texture can arise through more than one process. This study deals with the origin of coarse sieve-textured volcanic plagioclase (Fig. 1) in the light of new experimental observations and petrographic characteristics of resorbed natural plagioclase.

We interpret the texture of the plagioclase in Figure 1 as representing the remnants of an interconnecting network of channels, developed as the crystal underwent dissolution in response to physical and chemical changes in the magma reservoir or conduit. Initially, dissolution allowed diffusive and convective communication of the liquid in the channels with the bulk of the melt. However, in many volcanic rocks, sieve-textured plagioclase has euhedral rims that may result from subsequent crystal growth in response to loss of volatiles or cooling prior to eruption. If the rims encapsulate the crystal, this may leave the resorbed plagioclase with entrained liquid inclusions that have no obvious means of communication with the bulk of the magma. Upon extrusion, quenching of the magma leaves the network of channels filled with microcrystalline or glassy melt inclusions.

One interpretation of coarse sieve textures similar to those in Figure 1 is rapid skeletal growth resulting from undercooling (Kuo and Kirkpatrick, 1982). However, melt inclusions are commonly elongate parallel to, or abutted against, polysynthetic twin planes (Fig. 1), or they cut boundaries between individual crystals in glomerocrysts. Given that glomerocrysts and polysynthetic twin planes form after crystallization (Dungan and Rhodes, 1978), the cross-cutting relationships indicate that these textures must form by resorption rather than rapid crystallization.

Two other mechanisms have been proposed to explain the origin of sieve textures in plagioclase from volcanic rocks. They are magma mixing (e.g., Dungan and Rhodes, 1978; Tsuchiyama, 1985) and magmatic decompression (e.g., Vance, 1965; Stormer, 1972; Nelson, 1989). The possible effects of magma mixing have been experimentally investigated, although only under a limited set of conditions (Tsuchiyama, 1985). To date, these experiments have not produced textures like those in Figure 1, although future experiments may produce them if they are carried out under an expanded range of pressures, temperatures, and compositions. Many studies have shown the widespread occurrence of magma mixing as a petrogenetic process, and it is not our intent to dispute its importance. However, our results indicate that coarse sieve textures may result from the rapid ascent of magmas; therefore, invoking magma mixing solely on the basis of coarse sieve-textured plagioclase may not be warranted. In the absence of other criteria indicative of magma mixing, such as trapped liquid enclaves, disequilibrium phenocryst assemblages (e.g., Mg-rich olivine + quartz), or other chemical and isotopic criteria, magmatic decompression is a geologically simpler model, as it does not require an open system. However, the two processes need not be mutually exclusive. Both mechanisms desta-

---

* Present address: P.O. Box 1139, Pecos, New Mexico 87552, U.S.A.

0003–004X/92/1112–1242$02.00

bilize relatively sodic plagioclase, and all magmas decompress during ascent.

Magma mixing

Some of the relative merits of magma mixing and magmatic decompression models can be evaluated by a review of pertinent phase equilibria and experimental studies. Tsuchiyama's experiments model a mafic magma mixing with a more silicic, sodic plagioclase–bearing melt, which superheats and destabilizes the sodic plagioclase (Tsuchiyama, 1985). Any calcic plagioclase in the mafic magma would be supercooled, leaving a compositionally bimodal population of plagioclase crystals.

Mixing experiments produced dusty calcic mantles surrounding sodic cores (see Fig. 2 of Tsuchiyama, 1985), an effect produced by diffusional exchange between plagioclase and melt, assisted by the development of microchannels in the partially resorbing mantle. However, Tsuchiyama noted that his results did not produce the coarse sieve textures seen in Figure 1, which are similar to textures ascribed to magma mixing (see Fig. 5 of Dungan and Rhodes, 1978). Although it is apparent that some disequilibrium textures in lavas may result from the mixing of magmas, it seems that coarse sieve textures may also form by decompression.

Magmatic decompression

Plagioclase phase equilibria provide a framework for predicting the possible effects of rapid magmatic decompression and for designing experiments to model it. In Figure 2a, decompression of the bulk composition, represented by the filled squares, from A to B drives the system toward a more calcic plagioclase composition and a greater proportion of liquid, as represented by the relative lengths of the tie lines connecting A and B to the solidi and liquidi. Our experiments were designed to mimic this effect and to test whether rapid decompression can produce resorption in volcanic plagioclase phenocrysts. The vigor with which a decompressing plagioclase-bearing system begins to reequilibrate depends upon the magnitude and rate of pressure release. Decompression experiments modeled ascent rates ≥10 m/s ($\mathrm{d}P/\mathrm{d}t \geq 0.2$ kbar/min) over absolute pressure intervals of 2, 4, and 6 kbar.

The compositional changes produced by decompression in the binary system (Fig. 2a) are not large. However, the effects of additional components in decompressing systems can be evaluated in Figure 2b. The curves represent the plagioclase loop with coprecipitating diopside in the system Di-Ab-An. For decompression intervals of equal magnitude, the simultaneous dissolution of diopside produces a greater change in the equilibrium composition of plagioclase and a greater proportion of liquid at the final pressure than in the system Ab-An (Fig. 2a). The increased sensitivity of the system Di-Ab-An to changes in pressure and temperature results from the lower slopes of the plagioclase liquidus and solidus in both *P-X* and *T-X* projections caused by the coprecipitation of diopside (Wyllie, 1963). Thus, additional components and crystallizing phases in natural systems may enhance resorption effects caused by decompression. Our experimental data and those of Meen (1987) confirm that, under nearly isothermal conditions, increasing pressure decreases the An content of plagioclase in multicomponent natural systems (Fig. 3). This agrees with the observations of other workers (Green and Ringwood, 1967, 1968; Cohen et al., 1967) and supports our model for decompression-induced dissolution of plagioclase phenocrysts.

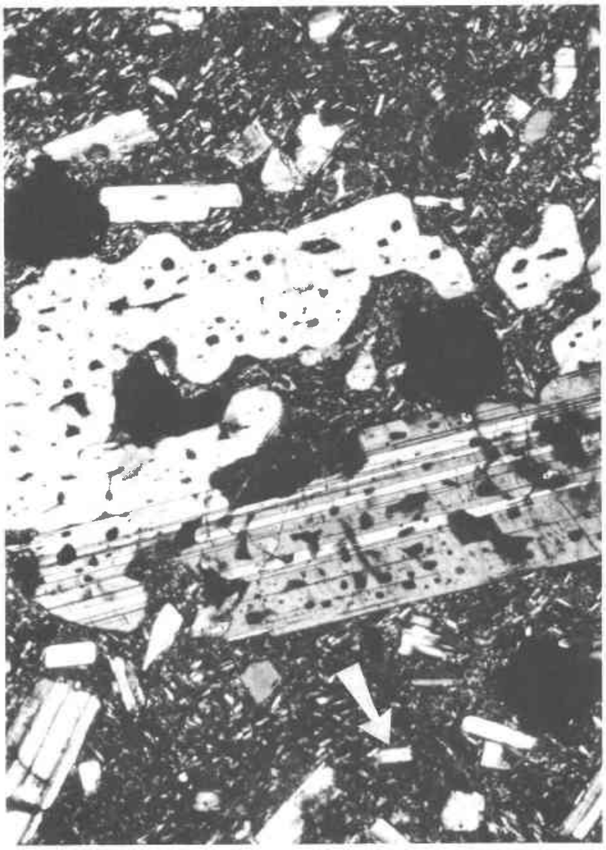

Fig. 1. Photomicrograph of the starting material containing large resorbed plagioclase phenocrysts typical of many intermediate and mafic lavas. Arrow indicates a member of a second population of euhedral, often more calcic, plagioclase microphenocrysts.

Although the curves in Figure 2 are for dry systems, no magma is strictly anhydrous, making it necessary to evaluate briefly the effects of volatiles. It is necessary to keep in mind that the process of magmatic decompression we describe is rapid, precluding a significant increase in volatile pressure due to crystallization of an anhydrous assemblage. Therefore, it is important to consider: (1) the effects of decompression on vapor-undersaturated systems, (2) the effects of decompression on vapor-saturated systems, and (3) volatile loss.

H_2O lowers the temperature of the liquidi and especially the solidi, but it does not significantly change the over-

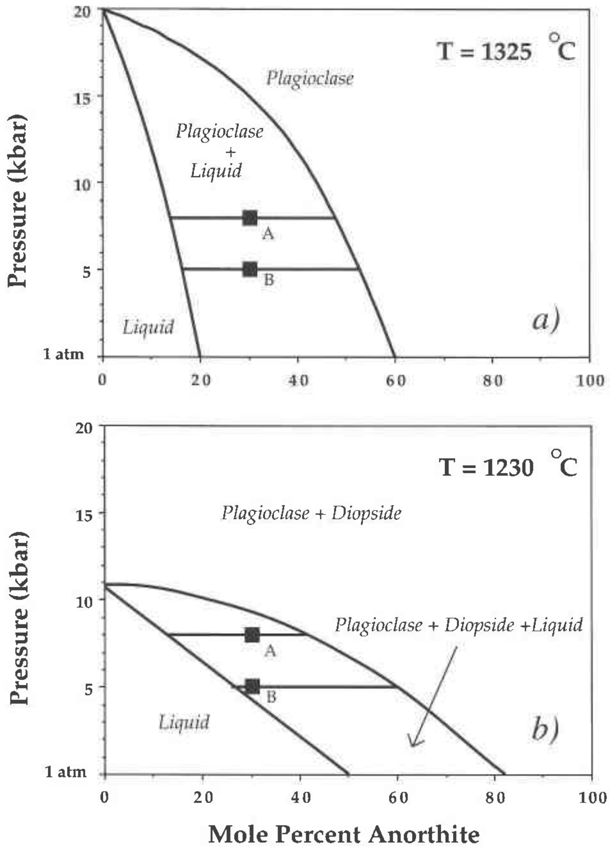

Fig. 2. (**a**) *P-X* section of the Ab-An system at 1325 °C (see Morse, 1980, Fig. 18.8). (**b**) *P-X* section of the pseudobinary plagioclase loop at about 1230 °C in the system Di-Ab-An constructed by moving the 1-atm loop up 100 °C to approximate its position at 10 kbar. This is a reasonable assumption, especially for the An-rich side of the diagram (see Morse, 1980, Figs. 18.6, 18.9). A given isothermal pressure drop produces a greater change in the composition and proportion of liquid in the system Di-Ab-An than in the system Ab-An.

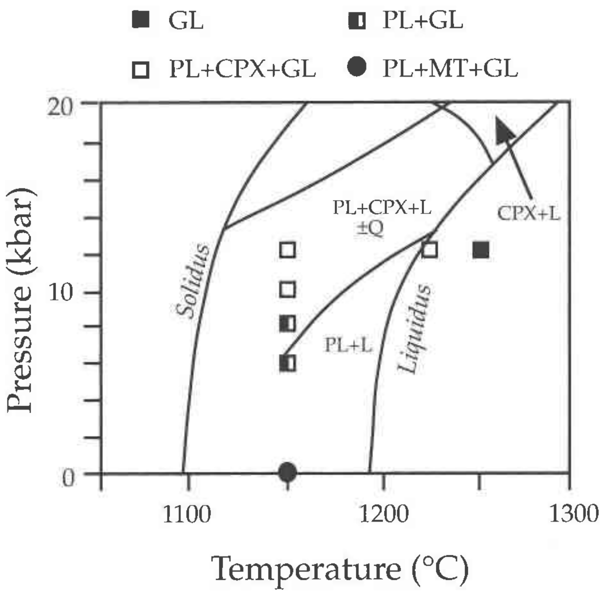

Fig. 3. *P-T* projection for andesite melts modified from Green (1972). Experimental phase assemblages from this study are also plotted for comparative purposes. Symbols the same as in Table 2.

all slope of the *P-X* and *T-X* loops when projected from H_2O. Thus, moderate volatile contents do not affect the general phase relationships described in Figure 2, as long as the magma does not become vapor saturated and degas. The presence of H_2O will assist decompression-induced resorption by reducing viscosity of the magma, which permits increased ascent and diffusion rates. Decompression of a vapor-saturated magma would hinder resorption if it causes the system to approach a negatively sloping solidus in *P-T* space—a condition likely to prevail at crustal pressures. On the other hand, the rapid loss of volatiles during eruption will arrest resorption by elevating the system's solidus temperature. Gradual volatile loss could induce a shift in plagioclase composition toward the Ab end-member and induce crystallization, thereby tending to counteract the effects of decompression. However, it is difficult to envision that this is an important process, except in very shallow magma reservoirs. Most mafic-intermediate orogenic magmas are not sufficiently H_2O-rich (<3 wt%) to exsolve a separate vapor phase until they ascend to less than 2–3 km from the Earth's surface (Gill, 1981). Therefore, as intermediate magmas rise through the crust, they are neither sufficiently H_2O-rich to approach a negatively sloping solidus, nor likely to lose volatiles in transit until they reach very shallow levels.

EXPERIMENTAL PROCEDURE AND RESULTS

Methods

The starting material (Table 1) was a high-K andesite from east-central Utah containing phenocrysts of plagioclase, clinopyroxene, orthopyroxene, and olivine, but lacking primary hydrous phases (Nelson, 1989). Liquidus and solidus curves are well constrained because of a compositional similarity to other experimentally investigated andesites (Green and Ringwood, 1968; Green, 1972; Meen, 1987) (Table 1). High-pressure experiments were conducted in a piston-cylinder apparatus with a furnace assembly 2.54 cm in diameter, similar to that described by Boettcher et al. (1981). The starting material was sealed inside Pt capsules, which in turn were sealed within capsules containing hematite. The HM buffer was used to minimize Fe loss to Pt and to maintain anhydrous conditions. Nonetheless, moderate Fe loss did occur (4–4.5 wt%). Experiments at atmospheric pressure employed a CO/CO_2 gas-mixing furnace near the value of the HM buffer. Temperatures were monitored with $Pt\text{-}Pt_{90}Rh_{10}$ thermocouples.

We conducted two sets of experiments. The first set established the equilibrium phase assemblages and com-

TABLE 1. Comparison of the compositions of starting materials

	1	2	3	4
SiO_2	56.08	55.58	56.40	59.72
TiO_2	0.94	0.88	1.40	0.68
Al_2O_3	16.98	17.39	16.60	16.82
FeO	9.14	8.28	8.70	6.30
MnO	0.13	na	0.10	0.13
MgO	2.85	4.82	4.30	3.10
CaO	5.99	7.13	8.50	7.16
Na_2O	3.36	3.81	3.00	3.99
K_2O	3.30	2.11	1.00	1.28
P_2O_5	0.38	na	na	0.20
Total	99.16	100.0	100.0	99.39

Note: na = data not available. Numbers 1–4 designate the following: 1 = starting material for this study (sample Gey-2, Nelson, 1989); 2 = Meen (1987) sample 2085; 3 = Green and Ringwood (1968) basaltic andesite; 4 = Green (1972) sample 68-66.

TABLE 2. Results and conditions of experiment set 1

P (kbar)	*T*(°C)	Duration (h)	Phases*
12	1250	24	GL
12	1225	24	GL, PL, CPX
12	1150	48	GL, PL, CPX
10	1150	48	GL, PL, CPX
8	1150	48	GL, PL
6	1150	48	GL, PL
1 atm	1150	96	GL, PL, MT

Note: All experiments were conducted with the HM buffer to minimize Fe loss to the capsule and keep the assemblage anhydrous. Temperature was monitored using a $Pt-Pt_{90}Rh_{10}$ thermocouple.

* GL = glass; PL = plagioclase; CPX = clinopyroxene; MT = magnetite.

positions at atmospheric pressure and 6, 8, 10, and 12 kbar (Table 2). All experiments were at 1250 °C for the first 24 h (above the liquidus at all pressures) to ensure complete melting of the crystalline starting material before subsequent crystallization; they were then rapidly cooled to 1150 °C (between the liquidus and solidus at all pressures).

We designed the second set of experiments to model magmatic decompression (Table 3). The experiments were held at 12 kbar and 1250 °C for 24 h to completely melt the starting material. The temperature was rapidly dropped isobarically to 1150 °C for another 24 h to partially crystallize the liquid. For each experiment, the pressure was then dropped either 2, 4, or 6 kbar and held for 3–12 h. This was accomplished for 2- and 4-kbar intervals by releasing piston pressure at a rate of approximately 0.2 kbar/min. Because of thermocouple failure, experiments at 6-kbar intervals were reloaded into new furnace assemblies and processed again at 6 kbar. Decompression rates were limited by the speed at which piston pressure could be released without thermocouple failure.

Pressure dependence of plagioclase composition

The first set of experiments establishes the phase relationships as a function of pressure. However, phase compositions and the crystallization sequence also depend on f_{O_2} (Hamilton et al., 1964). Because the experiments were carried out under very oxidizing conditions, our results may reflect a different crystallization sequence and range of mineral stabilities from those experienced in nature. Our experiments are generally consistent with the experimentally determined phase relationships of andesitic melts (Fig. 3). However, the liquidus temperature at 12 kbar of our starting material is somewhat higher than that of Green (1972) and the stability of clinopyroxene in our experiments is also limited to somewhat higher pressures (Fig. 3).

Microprobe analyses show that plagioclase is more Ab rich at increased pressure (Fig. 4). Plagioclase composition varies from about An_{57} to An_{37} between atmospheric pressure and 12 kbar. Ab and An contents vary at different rates because of the Or component, which increases from 4 to 8 mol% between 1 atm and 12 kbar. Despite considerable scatter in the data, it appears that the composition of plagioclase may change most rapidly as a function of pressure when coprecipitating with diopside (Fig. 4). This observation is consistent with the increased pressure dependence of plagioclase and liquid compositions when coprecipitating with diopside in the system Di-Ab-An (Fig. 2b) vs. the binary system (Fig. 2a). This probably results from rapid chemical changes in the liquid brought on by the coprecipitation or resorption of clinopyroxene with plagioclase. Although both clinopyroxene and plagioclase are increasingly soluble under isothermal conditions as pressure decreases, clinopyroxene becomes unstable at pressures less than about 8–10 kbar (Fig. 3). Therefore, at pressures approaching the stability limit of clinopyroxene, the liquid becomes enriched in Ca as the ratio of clinopyroxene to plagioclase rapidly decreases. This allows the crystallization of more calcic plagioclases.

Development of resorption textures

The results of the second set of experiments confirm that coarse sieve textures in volcanic rocks can be gen-

TABLE 3. Results and conditions of experiment set 2

P interval* (kbar)	Duration** (h)	Effect on plagioclase and other phases
2 (12-10)	60 (12)	Approx. 10% resorption. A few resorption channels per unit volume† in PL.
4 (12-8)	60 (12)	Approx. 30% resorption. Up to tens of resorption channels per unit volume.
4 (12-8)	52 (4)	Approx. 10% resorption. Up to tens of resorption channels per unit volume.
6 (12-6)	60 (12)	Nearly complete resorption of PL. New euhedral calcic PL.
6 (12-6)	54 (6)	Approx. 30% resorption. Up to hundreds of resorption channels per unit volume. Pseudomorphic MT after CPX.
6 (12-6)	51 (3)	Numerous resorption channels in PL. CPX becoming opaque.

* Numbers in parentheses indicate the initial and final pressures.

** Number in parentheses indicates the duration of the experiment at the final pressure.

† Degree of resorption and number of channels estimated for a cubic unit volume 100 μm in length per side.

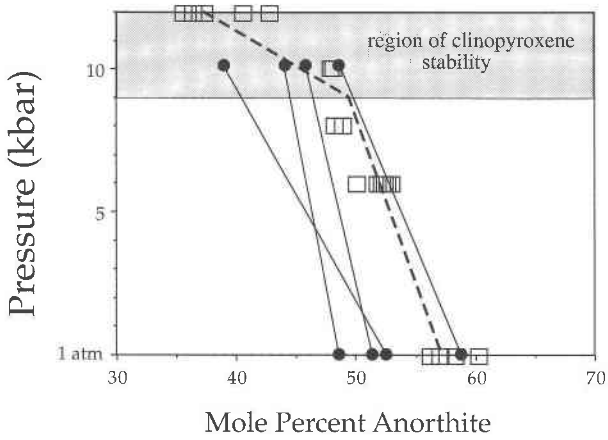

Fig. 4. Composition of plagioclase experiment products (open squares) as a function of pressure in terms of mole percent An, as determined by electron microprobe. Data from Meen (1987) (filled circles) are shown for comparative purposes where tie lines join plagioclase compositions from four starting materials under nearly isothermal (~1150 °C) conditions. Dashed line illustrates that the change in plagioclase composition may vary more strongly with pressure when clinopyroxene is stable.

erated by rapid decompression (Fig. 5). In terms of minimum time and pressure increments, sieve textures appear after decompressions of 2 kbar and 12 h, and after 4-kbar decompressions of just 4 h. The plagioclase crystals contain a mosaic of melt inclusions and dissolution channels strikingly similar to those in natural samples (compare Figs. 1 and 5).

The 6-kbar decompression experiments revealed a two-stage breakdown of clinopyroxene as the samples were decompressed to well below its stability limit. The breakdown of clinopyroxene, in a sequence of experiments where postdecompression conditions lasted 3, 6, and 12 h (Table 3), began as metastable Fe-Ti oxides nucleate in the clinopyroxene, rendering it opaque. After 6 h, pseudomorphic aggregates of oxide after clinopyroxene were dispersed throughout the liquid. After 12 h, essentially all crystalline phases had resorbed into the melt, and a few new, relatively calcic plagioclase crystals were growing in the liquid.

The nature of resorption in plagioclase depends on a number of factors. The number of channels per unit volume increases rapidly with the magnitude of the pressure interval, and the percentage of crystal resorbed increases with time (Table 3). For decompression intervals of 6 kbar, the density of resorption channels exceeds that which

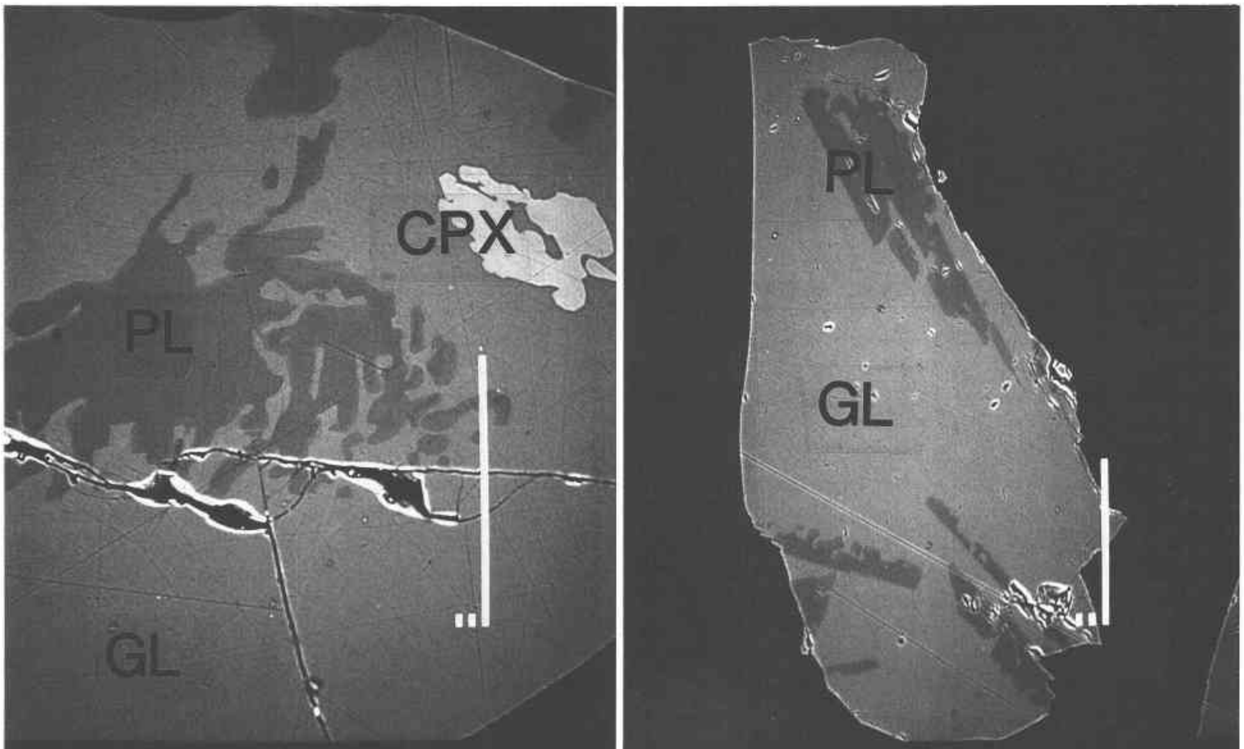

Fig. 5. Backscattered electron images of experiment products produced by a 4-kbar pressure drop of 12 h. Note the resorption in both plagioclase and clinopyroxene. Symbols the same as in Table 2. Large scale bars are 100 μm.

is commonly found in orogenic lavas. The dissolution of clinopyroxene may be important in the development of resorption textures in plagioclase, as its increased solubility and disappearance at lower pressures (Fig. 3) cause rapid changes in the composition of the melt that help drive resorption. We envision that a range of disequilibrium textures could develop in plagioclase in response to decompression rates that vary from exceedingly rapid to the infinitely slow rate required to produce equilibrium melting. These textures might include reverse zoning in addition to resorption. However, slow ascent rates would favor magmatic heat loss, which, in turn, would tend to counteract the effects of decompression.

DISCUSSION

Our experimental procedure involves three assumptions in relation to the magmatic processes being modeled. First, decompression rates and intervals are reasonable analogues of natural conditions. Second, heat loss is insignificant compared with the decompression rate, such that the process is nearly adiabatic. Third, over the pressure intervals considered, adiabatic decompression is nearly isothermal—otherwise significant cooling will counteract the effects of decompression. On the other hand, raising the temperature of the system by magma mixing will promote dissolution of plagioclase. However, we will consider the case of decompression without magma mixing.

In regard to the third assumption, adiabatic cooling must be less than the depression of the plagioclase liquidus caused by decompression. A liquid of composition $Ab_{33}An_{33}Di_{33}$ at 1425 °C has an adiabatic gradient of ~ 1.5 °C/kbar (calculated from Rivers and Carmichael, 1987), cooling the liquid just 3–9 °C for the pressure intervals (2–6 kbar) in this study. In a crystal-bearing magma, there is a second component to the total adiabatic gradient as latent heat is extracted from the liquid as the crystals resorb, resulting in further cooling of the system at equilibrium. Unlike the adiabatic gradient of a pure liquid, the extraction of latent heat is limited by the rate at which the crystals can resorb. Therefore, as long as resorption is incomplete, a rapidly decompressed magma is apt to be superheated with respect to its total adiabatic gradient.

Morse (1980) provided a convenient review of pertinent experimental data regarding the relative effects of isothermal decompression and adiabatic cooling. Albite has a liquidus with a slope of >10 °C/kbar, and the liquidus of intermediate plagioclase (An_{40}) is lowered by about 4 °C/kbar, about three times that of the liquid adiabat. However, as shown above, the effect of pressure is enhanced in multicomponent systems, whereas adiabatic gradients are not nearly as compositionally dependent. Morse (1980) reviewed data showing that the Di-An eutectic is lowered on the order of 10 °C/kbar. Gill (1981) noted that plagioclase is the liquidus phase in almost all andesites; thus, the whole rock liquidus represents a plagioclase liquidus, albeit independent of composition. At pressures less than 15 kbar, where plagioclase is on the liquidus and the liquidus is least sensitive to pressure, dT/dP is still about 5 °C/kbar (Green and Ringwood, 1968). In addition, Figure 2 shows that changing pressure also changes the equilibrium plagioclase composition, providing a further driving force for resorption. Therefore, we employed isothermal experiments as an approximation of natural processes, as the effect of pressure must be at least several times that of the adiabatic gradient.

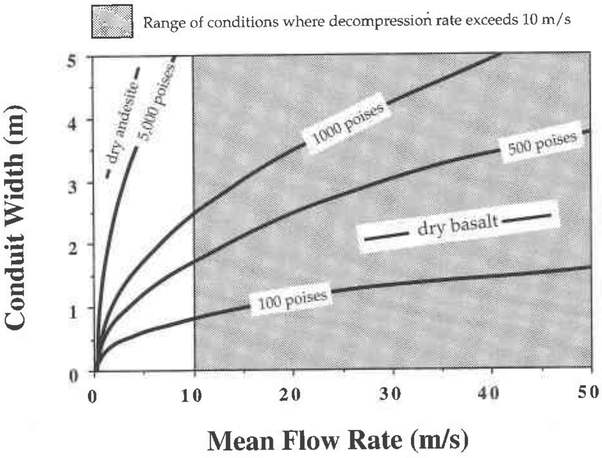

Fig. 6. Curves of mean flow rate or ascent rate of magma through a dikelike conduit as a function of conduit width and magma viscosity for a density contrast of 0.2 g/cm³ between the wall rock and magma (Kushiro, 1980, p. 117). Approximate values for dry andesite and basalt are shown for comparison. Note that ascent rates of >10 m/s (shaded region) are easily achieved for a reasonable range of geologic conditions in this model.

We produced strong resorption textures in plagioclase for decompression rates equivalent to rapid ascent rates (≥ 10 m/s). Therefore, resorption must also occur for a range of decompression rates less than this. Previous studies have determined magma ascent rates of up to 0.7 m/s for Mount St. Helens (Scandone and Malone, 1985) and 1.7 m/s beneath Kilauea (Klein et al., 1987), whereas Spera (1980) calculated minimum ascent rates of 0.5 m/s based upon the settling velocity of ultramafic nodules in basaltic magma. These data indicate that ascent rates in nature can be within at least an order of magnitude of our experimental rates.

Because the upper range of magmatic ascent rates may not be obvious to all, we constructed Figure 6 in order to evaluate possible ascent rates in magmatic systems with established conduits. Figure 6 is intended to illustrate the approximate scale (order of magnitude) of potential magma ascent rates: It is not a rigorous model. We assume the flow of a Newtonian fluid through a dikelike conduit, where the viscosities and density contrast between magma and wall rock used to derive the curves were treated as constants, although they vary somewhat with pressure (Kushiro, 1980). A model calculated for a tabular, rather than a cylindrical conduit, geometry provides a more

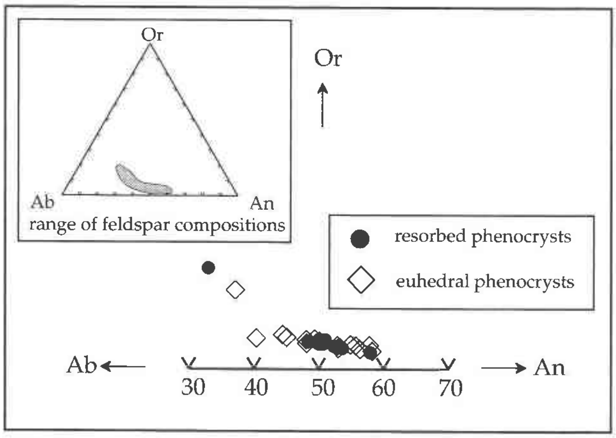

Fig. 7. Compositions of coexisting euhedral and resorbed phenocryst interiors from the lava in Figure 1.

conservative estimate of ascent rates because it takes into account the larger component of frictional resistance between the magma and wall rock.

The details of the calculation of the curves (Fig. 6) are only modestly dependent on the model. Magma ascent rates in conduits of varying geometry (e.g., Spera, 1980, p. 280–281; Kushiro, 1980, p. 117) are proportional to the density contrast and inversely proportional to the viscosity. However, ascent rates are also proportional to the square of the conduit width or radius, depending upon the geometry, causing this term to dominate the model. As a result, the calculations vary only by a factor of about 2–3, given reasonable variations in the density contrast (0.2–0.3 g/cm^3) independent of conduit geometry. Therefore, it appears that magma ascent rates may be very rapid, approaching our decompression rates over a range of geologically reasonable conditions. Magmas always contain a volatile component, and modest concentrations of H_2O (0.25 wt%) and CO_2 (0.5 wt%) can result in the reduction of viscosity by an order of magnitude in silicate liquids (White and Montana, 1990), thereby enhancing ascent rates.

Observations for natural systems

Our experimental results provide a basis for interpreting magmatic processes in volcanic rocks containing coarse sieve-textured plagioclase. The phenocrysts in Figure 1 are, on average, 10–20 times larger in section than those in our experiments, which develop similar textures after 4–12 h. If resorption scales linearly with crystal size, these textures may develop within a few days for large volcanic phenocrysts, following depressurization of at least 2–3 kbar.

The lava in Figure 1 is strongly porphyritic, with plagioclase phenocrysts occurring in two distinct populations: (1) resorbed crystals, and (2) euhedral phenocrysts. The phenocrysts show a fairly continuous size distribution up to a few millimeters, although the resorbed phenocrysts are always the largest crystals in the rock. Compositional profiles in the resorbed crystals are quite complex, exhibiting normal, reverse, and oscillatory zoning. The euhedral phenocrysts never approach the size of the large resorbed crystals (<0.5 mm), and usually exhibit normal zoning, although reverse and rare oscillatory zoning are also present. We summarize the compositions of crystal interiors of both populations in Figure 7 to help interpret this sample. Despite a compositional overlap between resorbed and unresorbed plagioclase, small euhedral plagioclase phenocrysts tend to range to significantly more calcic compositions. One analysis of resorbed plagioclase is distinctly An-rich and may represent a Ca-rich sector in a zoned crystal.

Many of the compositional and textural aspects of the phenocrysts may be antecedent to those features imposed by decompression. Therefore, in light of our experiments, we outline a subset of the characteristics of the sample in Figure 1 that may result from rapid pressure release. We suggest that the large resorbed plagioclase samples represent partial crystallization of a magma at depth. Their subsequent resorption was initiated by pressure release accompanied by relatively little heat loss as the magma ascended to a shallow magma reservoir. As a result of this process, a coarse sieve texture was superimposed on the complex zoning patterns that had already been acquired by these crystals. Unfortunately, it is nearly impossible to quantify this process. The pressure at which the resorbed crystals formed is difficult to estimate without a suitable geobarometer. Even if a suitable geobarometer existed, the problem would not be solved because uncertainties in calculated pressures are often as large (~2–3 kbar) as the decompression interval required to produce sieve textures. Likewise, the ascent rate is equally difficult to estimate, as our experiments do not constrain the relationship between resorption textures and the rate of pressure release. However, if the equilibrium composition of plagioclase immediately prior to and after eruption could be determined, it might be possible to estimate the minimum increment of pressure release from Figure 4.

Although it is relatively easy to ascribe first-order features like coarse sieve textures to decompression, the explanation of other compositional and textural features is more tenuous. Perhaps the nucleation of euhedral calcic microphenocryst cores was in response to new conditions of equilibrium at a substantially reduced pressure, and normal zoning of these crystals may have been in response to subsequent cooling and evolution of the liquid, as reflected in their compositional variation (Fig. 7). On the other hand, the reversely zoned euhedral crystals are more problematic. They may reflect phenomena such as crystal growth in a continually ascending magma in which plagioclase compositions are increasingly calcic (Fig. 2), or crystallization under increasing H_2O pressure (Johannes, 1978) caused by the formation of an anhydrous crystal assemblage after decompression or by a number of other phenomena, as reviewed by Gill (1981). It is difficult to interpret the presence of both normal and reverse zoning in the euhedral phenocrysts from the same sample. Zoning in plagioclase is a complex problem, underscoring the problematic nature of inferring magmatic processes from plagioclase phenocryst textures (Gill, 1981).

In general, the nucleation of new calcic crystals, rather than calcic overgrowths on the sodic plagioclase, is necessitated by the concomitant dissolution of the sodic crystals. Instances may occur in which resorption is arrested as dissolution kinetics become sluggish when the system approaches its new equilibrium. The resorbed crystals could be subsequently rimmed by calcic plagioclase. Alternatively, degassing or cooling of the magma may also arrest resorption and allow the crystallization of Ab-rich rims. A variety of processes may operate in combination at different times and places within a magma body, giving rise to many of the complex textural features observed in the plagioclase of orogenic magmas.

ACKNOWLEDGMENTS

We thank the Geological Society of America for a grant to S.T.N. and the Division of Physical Sciences at UCLA for financial support to A.M. We thank our colleague Jon Davidson for his careful reading of an early version of the manuscript, and Robert Jones for assistance with the electron microprobe. We also thank Kathy Cashman, Allen Glazner, Robert Hildebrandt, James Myers, and Rosamond Kinzler for their constructive reviews. Institute of Geophysics and Planetary Physics contribution number 3438.

REFERENCES CITED

Boettcher, A.L., Windom, K.E., Bohlen, S.R., and Luth, R.W. (1981) Low friction, anhydrous, low- to high-temperature furnace sample assembly for piston-cylinder apparatus. Reviews of Scientific Instruments, 52, 1903–1904.

Cohen, L.H., Ito, K., and Kennedy, G.C. (1967) Melting and phase relations in an anhydrous basalt to 40 kilobars. American Journal of Science, 265, 475–518.

Dungan, M.A., and Rhodes, M.J. (1978) Residual glasses and melt inclusions in basalts from DSDP legs 45 and 46: Evidence for magma mixing. Contributions to Mineralogy and Petrology, 67, 417–431.

Gill, J.B. (1981) Orogenic andesites and plate tectonics, 390 p. Springer-Verlag, New York.

Green, D.H., and Ringwood, A.E. (1967) The genesis of basaltic magmas. Contributions to Mineralogy and Petrology, 15, 103–190.

Green, T.H. (1972) Crystallization of calc-alkaline andesite under controlled high-pressure hydrous conditions. Contributions to Mineralogy and Petrology, 34, 150–166.

Green, T.H., and Ringwood, A.E. (1968) Genesis of the calc-alkaline igneous rock suite. Contributions to Mineralogy and Petrology, 18, 105–162.

Hamilton, D.L., Burnham, C.W., and Osborn, E.F. (1964) The solubility of water and effects of oxygen fugacity and water content on crystallization in mafic magmas. Journal of Petrology, 5, 21–39.

Johannes, W. (1978) Melting of plagioclase in the system Ab-An-H_2O and Q-Ab-An-H_2O at P_{H_2O} = 5 kbar, an equilibrium problem. Contributions to Mineralogy and Petrology, 66, 295–303.

Klein, F.W., Koynagi, R.Y., Nakata, J.S., and Tanigawa, W.R. (1987) The seismicity of Kilauea's magma system. U.S. Geological Survey Professional Paper, 1350 (2), 1019–1185.

Kushiro, I. (1980) Viscosity, density, and structure of silicate melts at high pressures, and their petrological applications. In R.B. Hargraves, Ed., Physics of magmatic processes, p. 93–120. Princeton University Press, Princeton, New Jersey.

Kuo, L.C., and Kirkpatrick, R.J. (1982) Pre-eruptive history of phyric basalts from DSDP Legs 45 and 46: Evidence from morphology and zoning patterns in plagioclase. Contributions to Mineralogy and Petrology, 79, 13–27.

Meen, J.K. (1987) Formation of shoshonites from calcalkaline basalt magmas: Geochemical and experimental constraints from the type locality. Contributions to Mineralogy and Petrology, 97, 333–351.

Morse, S.A. (1980) Basalts and phase diagrams—An introduction to the quantitative use of phase diagrams in igneous petrology, 356 p. Springer-Verlag, New York.

Nelson, S.T. (1989) Geologic map of the Geyser Peak quadrangle, Sevier and Wayne Counties, Utah (geologic report included). Utah Geological and Mineral Survey Map Publication 114, scale 1:24000.

Rivers, M.L., and Carmichael, I.S.E. (1987) Ultrasonic studies of silicate melts. Journal of Geophysical Research, 92, 9247–9270.

Scandone, R., and Malone, S.D. (1985) Magma supply, magma discharge, and readjustment of the feeding system of Mount St. Helens during 1980. Journal of Volcanology and Geothermal Research, 23, 239–262.

Spera, F.J. (1980) Aspects of magma transport. In R.B. Hargraves, Ed., Physics of magmatic processes, p. 265–323. Princeton University Press, Princeton, New Jersey.

Stormer, J.C. (1972) Mineralogy and petrology of the Raton-Clayton volcanic field, northeastern New Mexico. Geological Society of America Bulletin, 83, 3299–3322.

Tsuchiyama, A. (1985) Dissolution kinetics of plagioclase in the melt system diopside-albite-anorthite, and origin of dusty plagioclase in andesites. Contributions to Mineralogy and Petrology, 89, 1–16.

Vance, J.A. (1965) Zoning in igneous plagioclase: Patchy zoning. Journal of Geology, 73, 637–651.

White, B.S., and Montana, A. (1990) The effect of H_2O and CO_2 on the viscosity of sanidine liquid at high pressures. Journal of Geophysical Research, 95, 15683–15693.

Wyllie, P.J. (1963) Effects of changes in slope occurring on liquidus and solidus paths in the system diopside-anorthite-albite. Mineralogical Society of America Special Paper, 1, 204–212.

MANUSCRIPT RECEIVED DECEMBER 30, 1991
MANUSCRIPT ACCEPTED JULY 13, 1992